STRUCTURAL INSTABILITY INDUCED BY ACTUATOR CONSTRAINTS IN CONTROLLED AEROELASTIC SYSTEM

Max Demenkov
Faculty of Computing Sciences and Engineering
De Montfort University
UK
demenkov@dmu.ac.uk

Abstract

In this paper, an active flutter control scheme is investigated for a 2dof airfoil with nonlinear torsional stiffness. We use a simple graphical method to characterize all possible system equilibria. With the help of this method we study how an active flutter suppression system can lead to "parasitic" steady states, which are different from the nominal zero-pitch, zero-plunge trim conditions. It appears that these equilibria can be induced by the presence of non-smooth saturation function, which describes amplitude constraints imposed on the system actuators. With control system built using only knowledge of "nominal" system dynamics, the closed-loop system becomes structurally unstable in the sense that a small change in its parameters or the addition of infinitesimal unmodeled dynamics can lead to the "parasitic" steady states appearance or disappearance.

Key words

Structural stability, non-smooth dynamical systems, control input constraints, active vibration control

1 Introduction

Active flutter suppression approach has been studied for many years to prevent catastrophic structural failure due to excessive vibrations in aeroelastic systems. Control surfaces such as spoilers and flaps have been generally used to generate auxiliary aerodynamic lift and moment, although some non-standard actuators, such as piezoelectric and jet reaction torquer, were also investigated.

In post-design analysis of flutter suppression methods the attention so far has been concentrated mainly on the limit cycle oscillations (LCO), as their prevention is the main goal of any such method. It is usually expected that the designed feedback stabilizes the closed-loop system around nominal zero-pitch, zero-plunge equilibrium. Nevertheless, due to the nonlinear nature of aeroelastic systems, it is theoretically possible that the feedback will induce in the closed-loop system new, undesirable stable or unstable trim conditions that are different from the nominal one. An unstable equilibrium can also be surrounded by a stable limit cycle having small amplitude or can change the system dynamics qualitatively in some other way. As a result, the closed-loop performance can degrade not only because of insufficient LCO prevention, but also because of undesirable equilibria that were created by the feedback itself (Goman and Demenkov, 2008).

Although this aspect of aeroservoelastic feedback design was not systematically studied before in the literature, one can find there a few examples of undesired attractors existence due to a particular form of feedback control. These examples are connected with the aeroelastic apparatus developed in Texas A&M University. The existence of a stable non-zero equilibria has been experimentally confirmed for the closed-loop system with one (Kurdila *et al.*, 2001) and two (Platanitis and Strganac, 2004) actuators under feedback linearization control. In both cases one cannot detect the "parasitic" attractors via the closed-loop model investigation. These effects were attributed by authors to inexact cancelation of the stiffness nonlinearity, unmodeled Coulomb friction, aerodynamic loading. The particular source of these problems was not, however, clear.

In this paper we propose an approach based on the notion of structural stability that can help to explain these effects, which seem to have an importance for the vibration control in general. For the illustration, we use the model given in (Platanitis and Strganac, 2004). We assume that the system parameters cannot be measured exactly and there are exist unknown dynamics, i.e. equations that govern the apparatus in nature but were not included in the system model due to simplification assumptions. We show that in some circumstances the controller, designed using only the knowledge of "nominal" system dynamics, can lead to unexpected changes in the dynamics of the closed-loop system if the real-life system even slightly differs from

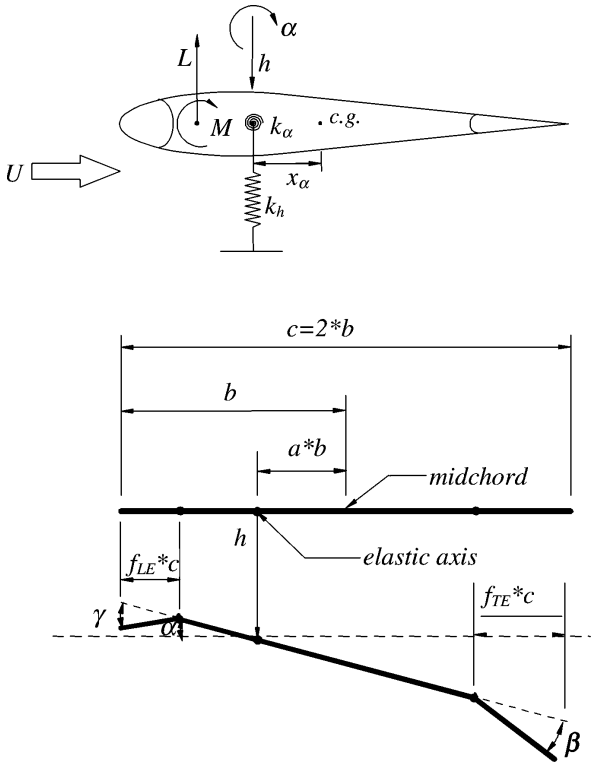

Figure 1. The aeroelastic system (courtesy of the American Institute of Aeronautics and Astronautics).

that used for the synthesis. The steady-states, which can randomly appear in the system in this case, are totally absent in the nonlinear model that is used for the closed-loop system design and simulation. However, with the proposed methodology it is possible to identify structurally unstable configurations without the exact knowledge of system dynamics.

2 System model

The equations of motion for a wing section with two degrees of freedom are taken here as in (Platanitis and Strganac, 2004):

$$\begin{bmatrix} m_T & m_W x_\alpha b \\ m_W x_\alpha b & I_\alpha \end{bmatrix} \begin{bmatrix} \ddot{h} \\ \ddot{\alpha} \end{bmatrix} + \begin{bmatrix} c_h \dot{h} \\ c_\alpha \dot{\alpha} \end{bmatrix} + \begin{bmatrix} F_h \\ M_\alpha \end{bmatrix} = \begin{bmatrix} -L(t) \\ M(t) \end{bmatrix}, \tag{1}$$

where h - the plunge displacement, α - the pitch angle, m_T - the total mass of pitch–plunge system, m_W - the total wing section plus mount mass, $F_h(h) = k_h h$ -the plunge force due to the plunge stiffness k_h, $M_\alpha(\alpha) = k_\alpha \alpha$ - the pitch moment due to the pitch stiffness k_α.

It is important to note that the sole source of nonlinearity in these equations arises from the polynomial model of the pitch stiffness (see Fig. 2):

$$k_\alpha(\alpha) = 12.77 + 53.47\alpha + 1003\alpha^2. \tag{2}$$

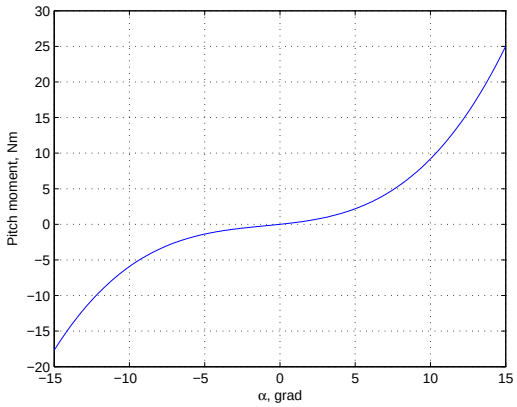

Figure 2. The pitch moment.

Using the nondimensional distance from midchord to elastic axis position a and the semichord of wing section b, we first compute the nondimensional distance from elastic axis to center of mass x_α and then distance r_{cg} (see Fig. 1):

$$x_\alpha = -(0.0998 + a), r_{\text{cg}} = b x_\alpha. \tag{3}$$

Viscous damping coefficients for plunge and pitch motion are represented in the equations by c_h and c_α, respectively. The total pitch moment of inertia about elastic axis I_α is computed as

$$I_\alpha = I_{\text{cam}} + I_{\text{cg-wing}} + m_{\text{wing}} r_{\text{cg}}^2, \tag{4}$$

where I_{cam} - pitch cam moment of inertia, $I_{\text{cg-wing}}$ - wing section moment of inertia about the center of gravity, m_{wing} - mass of wing section.

We assume that the quasi-steady aerodynamic force L and moment M are modeled as

$$\begin{aligned} L = {} & \rho U^2 b s \{ C_{l_\alpha} [\alpha + (\dot{h}/U) + (1/2 - a) b (\dot{\alpha}/U)] \\ & + C_{l_\beta} \beta + C_{l_\gamma} \gamma \}, \\ M = {} & \rho U^2 b^2 s \{ C_{m_{\alpha-\text{eff}}} [\alpha + (\dot{h}/U) + \\ & (1/2 - a) b (\dot{\alpha}/U)] + C_{m_{\beta-\text{eff}}} \beta + C_{m_{\gamma-\text{eff}}} \gamma \}, \end{aligned} \tag{5}$$

where ρ - air density, U - freestream velocity, s - wing section span, γ and β - leading- and trailing-edge control surface deflections.

The effective dynamic and control moment derivatives due to angle of attack ($C_{m_{\alpha-\text{eff}}}$) and trailing- and leading-edge control surface deflection ($C_{m_{\beta-\text{eff}}}$ and $C_{m_{\gamma-\text{eff}}}$, respectively) about the elastic axis are defined as follows:

$$\begin{aligned} C_{m_{\alpha-\text{eff}}} &= (1/2 + a) C_{l_\alpha} + 2 C_{m_\alpha}, \\ C_{m_{\beta-\text{eff}}} &= (1/2 + a) C_{l_\beta} + 2 C_{m_\beta}, \\ C_{m_{\gamma-\text{eff}}} &= (1/2 + a) C_{l_\gamma} + 2 C_{m_\gamma} \end{aligned} \tag{6}$$

Table 1. System parameters

Parameter	Value
ρ	1.225 kg/m^3
a	-0.6719
b	0.1905 m
s	0.5945 m
k_h	2844 N/m
c_h	27.43 kg/s
c_α	0.0360 kg·m^2/s
m_{wing}	4.340 kg
m_W	5.230 kg
m_T	15.57 kg
I_{cam}	0.04697 kg·m^2
$I_{\text{cg-wing}}$	0.04342 kg·m^2
C_{l_α}	6.757
C_{l_β}	3.774
C_{m_β}	-0.6719
C_{l_γ}	-0.1566
C_{m_γ}	-0.1005

where $C_{l_{\alpha,\beta,\gamma}}$ -lift and $C_{m_{\alpha,\beta,\gamma}}$ - moment coefficients per angle of attack and control surface deflections, respectively. Note that $C_{m_\alpha} = 0$ for a symmetric airfoil, as in our case.

The parameters of the model are given in Table 1.

Let us write the system in the following convenient form:

$$A\ddot{x} + B\dot{x} + C(\alpha)x = Du \tag{7}$$

where

$$x = \begin{bmatrix} h \\ \alpha \end{bmatrix}, u = \begin{bmatrix} \beta \\ \gamma \end{bmatrix}, A = \begin{bmatrix} m_T & m_W x_\alpha b \\ m_W x_\alpha b & I_\alpha \end{bmatrix},$$

$$B = \begin{bmatrix} c_h + \rho U b s C_{l_\alpha} & \rho U b^2 s C_{l_\alpha}(1/2 - a) \\ -\rho U b^2 s C_{m_\alpha - \text{eff}} & c_\alpha - \rho U b^3 s C_{m_\alpha - \text{eff}}(1/2 - a) \end{bmatrix},$$

$$C(\alpha) = \begin{bmatrix} k_h & \rho U^2 b s C_{l_\alpha} \\ 0 & k_\alpha(\alpha) - \rho U^2 b^2 s C_{m_\alpha - \text{eff}} \end{bmatrix},$$

$$D = \begin{bmatrix} -\rho U^2 b s C_{l_\beta} & -\rho U^2 b s C_{l_\gamma} \\ \rho U^2 b^2 s C_{m_\beta - \text{eff}} & \rho U^2 b^2 s C_{m_\gamma - \text{eff}} \end{bmatrix} \tag{8}$$

Now it is easy to write the system in the Cauchy form (note that the equations are given for α, β and γ in radians):

$$\begin{bmatrix} \dot{x} \\ \ddot{x} \end{bmatrix} = \begin{bmatrix} 0 & 0 & 1 & 0 \\ 0 & 0 & 0 & 1 \\ -A^{-1}C(\alpha) & & -A^{-1}B & \end{bmatrix} \begin{bmatrix} x \\ \dot{x} \end{bmatrix} + \begin{bmatrix} 0 & 0 \\ 0 & 0 \\ A^{-1}D & \end{bmatrix} u \tag{9}$$

The actuator deflections are subject to strong amplitude constraints:

$$-u_{max} \le \beta, \gamma \le u_{max}. \tag{10}$$

The controller given in (Platanitis and Strganac, 2004) is in the form of a simple nonlinear dynamic inversion:

$$u(x, \dot{x}) = D^{-1}[C(\alpha)x + B\dot{x} + A(K_x x + K_{\dot{x}}\dot{x})], \tag{11}$$

where

$$K_x = \begin{bmatrix} K_h & 0 \\ 0 & K_\alpha \end{bmatrix}, \quad K_{\dot{x}} = \begin{bmatrix} K_{\dot{h}} & 0 \\ 0 & K_{\dot{\alpha}} \end{bmatrix}. \tag{12}$$

Here we use a simplification in comparison with (Platanitis and Strganac, 2004) - we discard the adaptive terms of the control law.

The feedback gain pairs $K_h, K_{\dot{h}}$ and $K_\alpha, K_{\dot{\alpha}}$ are designed so that to stabilize the two-dimensional integrator with states $(h, \dot{h})$ or $(\alpha, \dot{\alpha})$, correspondingly. In the absence of control constraints, this design leads to the closed-loop system where dynamics for h and α are totally separated from each other. In the cited paper these gains where obtained via the linear-quadratic regulator synthesis (Skogestad and Postlethwaite, 1996).

Problems with this design arise, however, when control constraints (10) are active and the control system cannot cancel the nonlinear term anymore.

3 Equilibria analysis in a plane

It is obvious that at an equilibrium $\dot{x} = 0, \ddot{x} = 0$, and it follows from (7) that we only need to find all solutions of the following two nonlinear equations:

$$f(x) = A^{-1}(Du(x, 0) - C(\alpha)x) = 0, \tag{13}$$

where term $u(x, 0)$ corresponds to (11) with $\dot{x} = 0$ and also supplemented with the saturation function to take into account control constraints:

$$u(x, 0) = \text{sat}(D^{-1}[C(\alpha)x + AK_x x]). \tag{14}$$

Here sat() is the standard saturation function, defined for each component of its vector argument as:

$$\text{sat}(u) = \text{sign}(u) \min\{u_{max}, |u|\}.$$

In that regions of the plane (h, α) where both β, γ are unsaturated, we will not find any equilibria in the system that are different from the nominal one. It is therefore the regions were at least one of actuators is saturated, which should attract our attention.

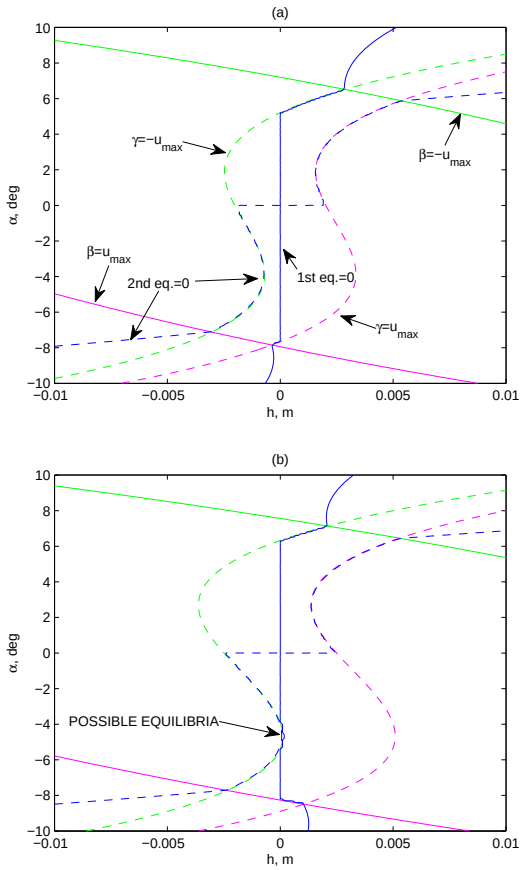

Figure 3. The pitch-plunge plane for U=18 and 20 m/s.

To visualize the solution of equation (13), we employ the standard function *contourc* in the MATLAB environment. We treat each equation in (13) as a function and then draw its zero level contour in the plane (h, α). Then, an intersection of these two curves gives us a solution of (13), i.e. a closed-loop system equilibrium. We also draw the curves corresponding to $\beta = \pm u_{max}$ and $\gamma = \pm u_{max}$. In this way we can divide the plane into saturated and unsaturated regions.

For the following example we took $u_{max} = 15^o$ and synthesized linear-quadratic regulator with identity weighting matrices, which gives us $K_h = K_\alpha = -1$. In Fig. 3, (a) all curves are shown for $U = 18$ m/s. Green and magenta curves correspond to extremal values of control function: solid to $\beta = \pm u_{max}$and dashed to $\gamma = \pm u_{max}$. Region that includes the origin and is overall bounded by these curves is the unsaturated region. Blue curves depict zeros of the first (solid) and the second (dashed) equation in (13). From the given picture it is clear that there are no other equilibria exist for $U = 18$ m/s except for the nominal one.

In the next picture (Fig. 3,(b)) the situation is changed with increase of the flow velocity U up to 20 m/s. In the vicinity of the arrow pointer one can see that zero curves for both equations are very close to each other, despite there is actually no intersection between them. It is reasonable to pose a question in this case about how small should be a perturbation of the system that could provoke an intersection of the curves.

4 Structural stability

The notion of structural stability was first introduced in (Andronov and Pontryagin, 1937). Informally, we say that a system is structurally stable if small variations in the model does not change qualitatively the set of trajectories originating from all initial conditions in the state space. This notion is of great importance in dynamical systems theory, since it is possible to define bifurcations in both smooth and non-smooth systems via the structural stability concept (di Bernardo *et al.*, 2008). Any dynamical system at bifurcation values of its parameters is structurally unstable (small variations of its dynamics can change the number and/or stability properties of steady states, limit cycles, etc.)

Structural stability has attracted attention for a long time since (Palis and Smale, 1970) conjectured that a smooth dynamical system is structurally stable if and only if it satisfies the so called *Axiom A* plus the strong transversality condition. A subclass of such systems is called *Morse-Smale* systems (Guckenheimer and Holmes, 1986). The non-wandering set of a Morse-Smale system is composed of a finite number of hyperbolic singularities and periodic orbits, whose stable and unstable manifolds intersect transversally.

For systems defined on two-dimensional manifolds the conjecture is contained in the classical work (Peixoto, 1962). For the general case, the result was proved independently in (Wen, 1996) and (Hayashi, 1997; Hayashi, 1999). For the recent discussion of the conjecture see also (Moriyasu *et al.*, 2001).

Despite the great interest attracted towards the structural stability in the pure mathematics community, one can hardly find real-life applications of the concept. The author aware only of four such papers (Pai *et al.*, 1995*a*; Pai *et al.*, 1995*b*; Kaslik and Balint, 2007; Sumida *et al.*, 2007) published relatively recently. The later paper noted that even any numerical degree of the structural stability was not defined previously. It is clear that engineering applications of the concept are of great interest in these circumstances. Could it be possible to accidentally create a system that is constantly situated at a verge of some bifurcation? A feedback provided for the structurally stable system might turn it into the opposite. This is the possibility that we try to confirm in this paper.

Even with the existing achievements in the theory of structural stability, on the first look we face difficulties applying the existing theory to our system. First, a proof that our system is not structurally stable seems not very easy, since it is multidimensional and in general case we need to study its invariant manifolds. Second, because of non-smooth control constraints, the existing theory is not directly applicable. In order to meet the smoothness requirement, one can use a smoothed version of the saturation function, which can

introduce some deviations in the system behaviour. It is also hard to study our system directly in the context of non-smooth dynamical systems theory (Simic *et al.*, 2001; Broucke *et al.*, 2001; Leine and Nijmeijer, 2004; di Bernardo *et al.*, 2008), since this theory is still in its beginning stages.

Fortunately, in our case we study much more simpler problem. The nature of it become more clear in Fig. 4, were $U = 22$ m/s. In the area catched by the ellipse one can see both zero curves following the boundary of unsaturated region with $\gamma = -u_{max}$. They are clearly going practically in parallel to each other. The picture is therefore indicating the *structural instability* in the closed-loop system. Despite there is still no intersection between the curves, with a very small change in the closed-loop dynamics one should expect the appearance of new equilibria in the system, which are impossible to observe in the model using only the nominal system dynamics. This is what probably happened in experiments (Kurdila *et al.*, 2001; Platanitis and Strganac, 2004). Note that the structural instability is caused by the actuator constraints, as there is no way for undesired equilibria to appear in the unsaturated region.

Since the steady states of our system are completely characterized by the zeros of two-dimensional vector function (13), we only need to show that this function is going to change the number of its zeros with any slight variations of the function.

We have generally two ways to achieve this - either change of the system parameters or introduction of some unmodeled dynamics. In the control theory the former corresponds to the *structured* and the later to the *unstructured* uncertainty (Skogestad and Postlethwaite, 1996).

Even if it is not possible to create an intersection of the curves by a small change in the system parameters, the introduction of some unstructured uncertainty can always create some fixed points in this area, and that is why we investigate this possibility below. From the physical nature of our problem (equations composed of moments and forces) it is reasonable to expect the unknown dynamics to be of additive type and therefore consider the addition of infinitesimal unknown function:

$$f_{mod}(x) = f(x) + g(x) \tag{15}$$

From the adopted definition of structural stability (Kuznetsov, 2004), our system is not structurally stable if $f_{mod}(x)$ has different number of zeros than $f(x)$ while they are C^1-close, i.e. norms of $g(x)$ and its first partial derivative are very small. The particular numerical definition of "small" is, of course, not so simple and should be better judged by those who perform real-life experiments.

It is possible to numerically solve the equation $f_{mod}(x) = 0$ in some pitch-plunge range to find any

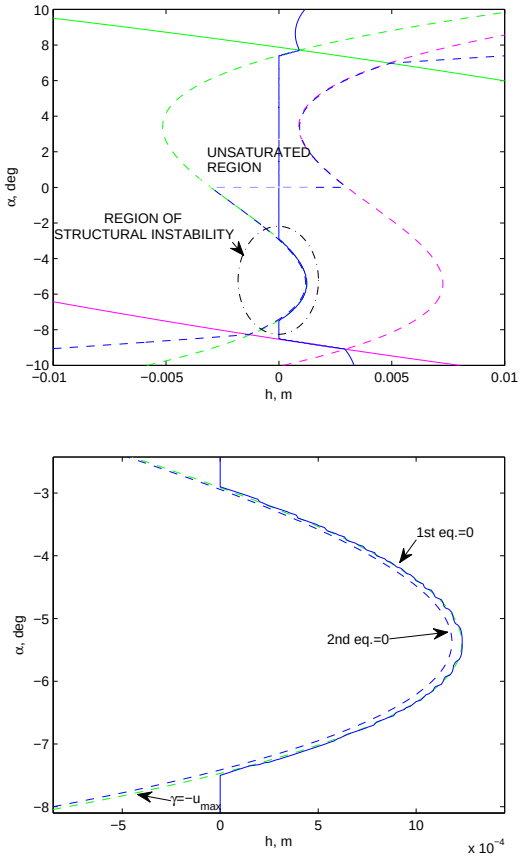

Figure 4. The pitch-plunge plane for U=22 m/s.

$g(x)$ with a minimum possible norm. The particular value of this norm might serve as a numerical measure of structural instability.

As an example, let us artificially create a linear-type $g(x)$ so that it produces a steady-state. We pick the point $h = 0.001636157$ m, $\alpha = -0.1000768$ rad in the middle of the structural instability region for $U = 22$ m/s. After that, we have to solve the following equations:

$$g(x) = Gx = \begin{bmatrix} g_{11}h & g_{12}\alpha \\ g_{21}h & g_{22}\alpha \end{bmatrix} = -f(x) = \begin{bmatrix} -0.0048 \\ -0.0054 \end{bmatrix} \tag{16}$$

To minimize the coefficients of our unmodeled dynamics, we use the formula for the minimum distance from the origin in (g_{i1}, g_{i2}) -plane to lines $g_{i1}h + g_{i2}\alpha = -f_i$:

$$g_{i1} = \frac{-f_i h}{h^2 + \alpha^2}, \quad g_{i2} = \frac{-f_i \alpha}{h^2 + \alpha^2}, \quad i = 1, 2. \tag{17}$$

The hypothetical unmodeled dynamics in this case is given by

$$Gx = \begin{bmatrix} -0.0008h & 0.0479\alpha \\ -0.0009h & 0.0538\alpha \end{bmatrix} \tag{18}$$

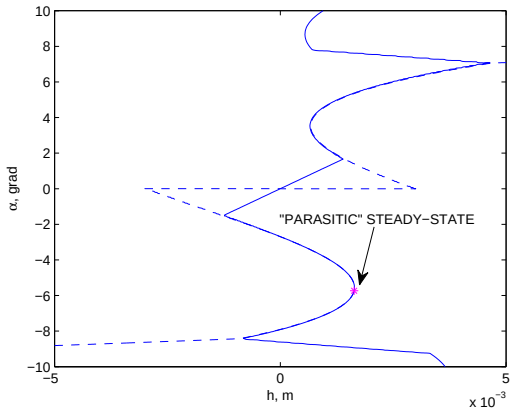

Figure 5. The "parasitic" steady-state created by the hypothetical unmodeled dynamics.

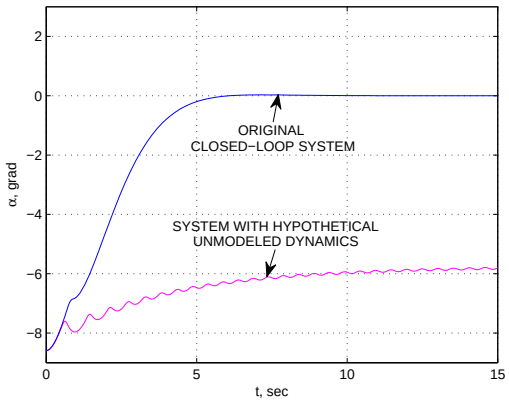

Figure 6. Simulation results with (magenta) and without (blue) the unmodeled dynamics.

To understand how small is that, one can compare it to the corresponding open-loop nominal dynamics, given by

$$-A^{-1}C(\alpha)x = \begin{bmatrix} -214.1395h & -24.3894\alpha \\ 859.9288h & -129.7758\alpha \end{bmatrix} \quad (19)$$

Despite being insignificant while considering the open-loop model, with the addition of the hypothetical dynamics to the closed-loop equations like

$$A\ddot{x} + B\dot{x} + C(\alpha)x - AGx = Du \quad (20)$$

it will produce a new steady-state at $h = 0.001636157$ m, $\alpha = -0.1000768$ rad, $\dot{h} = \dot{\alpha} = 0$, shown by magenta point in Fig. 5. Blue curves correspond to zeros of the first (solid) and the second (dashed) component of $f_{mod}(x)$.

To find out stability properties of the artificially created equilibrium, we perform simulation of the closed-loop system with and without the hypothetical unmodeled dynamics. The results of time integration using MATLAB function *ode45* with the initial conditions $h = 0.001$ m, $\alpha = -0.15$ rad, $\dot{h} = \dot{\alpha} = 0$ clearly show that the equilibrium is stable (see Fig. 6 for the magenta plot of α vs. time). The "nominal" system, simulated from the same initial condition, at the same time tends to the zero origin. Therefore, in an experiment the system could stabilize itself at some nonzero position, despite one cannot expect it even from very extensive simulations or any theoretical analysis of the original system.

5 Conclusion

A simple graphical method has been used to reveal structural instability arising in a closed-loop aeroelastic system under amplitude actuator constraints. The theoretical explanation is proposed for some "mystical" experimental results appeared in the literature previously. The result points out to the importance of structural stability in the active vibration suppression problem. The proposed methodology identifies regions of structural instability and can help in practical regulator design.

References

Andronov, A. and L. Pontryagin (1937). Systemes grossiers. *Dokl. Akad. Nauk SSSR* **14**, 247–251.

Broucke, M., C.C. Pugh and S.N. Simic (2001). Structural stability of piecewise smooth systems. *Computational and Applied Mathematics* **20**(1–2), 51–90.

di Bernardo, M., C.J. Budd, A.R. Champneys and P. Kowalczyk (2008). *Piecewise-smooth dynamical systems: theory and applications*. Vol. 163 of *Applied Mathematical Sciences*. Springer. London.

Goman, M.G. and M.N. Demenkov (2008). Multiple attractor dynamics in active flutter suppression problem. In: *Proceedings of the ICNPAA 2008: Mathematical Problems in Engineering, Aerospace and Sciences*. Genoa, Italy.

Guckenheimer, J. and P. Holmes (1986). *Nonlinear oscillations, dynamical systems, and bifurcations of vector fields*. Vol. 42 of *Applied Mathematical Sciences*. Springer-Verlag. New York.

Hayashi, S. (1997). Connecting invariant manifolds and the solution of the C^1 stability and ω-stability conjectures for flows. *Annals of Mathematics* **145**, 81–137.

Hayashi, S. (1999). Correction to "Connecting invariant manifolds and the solution of the C^1 stability and ω-stability conjectures for flows". *Annals of Mathematics* **150**, 353–356.

Kaslik, E. and S. Balint (2007). Structural stability of simplified dynamical system governing motion of ALFLEX reentry vehicle. *Journal of Aerospace Engineering* **20**(4), 215–219.

Kurdila, A.J., T.W. Strganac, J.L. Junkins, J. Ko and M.R. Akella (2001). Nonlinear control methods for high-energy limit-cycle oscillations. *Journal of Guidance, Control, and Dynamics* **24**(1), 185–192.

Kuznetsov, Y.A. (2004). *Elements of Applied Bifurcation Theory*. Springer. New York.

Leine, R. and H. Nijmeijer (2004). *Dynamics and Bifurcations of Non-Smooth Mechanical Systems*. Vol. 18 of *Lecture Notes in Applied and Computational Mechanics*. Springer-Verlag. Berlin.

Moriyasu, K., K. Sakai and N. Sumi (2001). Vector fields with topological stability. *Transactions of the American Mathematical Society* **353**(8), 3391–3408.

Pai, M.A., P.W. Sauer and B.C. Lesieutre (1995*a*). Static and dynamic nonlinear loads and structural stability in power systems. *Proceedings of the IEEE* **83**(11), 1562–1572.

Pai, M.A., P.W. Sauer, B.C. Lesieutre and R. Adapa (1995*b*). Structural stability in power systems - effect of load models. *IEEE Transactions on Power Systems* **10**(2), 609–615.

Palis, J. and S. Smale (1970). Structural stability theorems. In: *Global analysis, Proc. Sympos. Pure Math.*. Vol. 14. pp. 223–231. Amer. Math. Soc.. Providence.

Peixoto, M.M. (1962). Structural stability on two-dimensional manifolds. *Topology* **1**, 101–120.

Platanitis, G. and T.W. Strganac (2004). Control of a nonlinear wing section using leading- and trailing-edge surfaces. *Journal of Guidance, Control, and Dynamics* **27**(1), 52–58.

Simic, N., K.H. Johansson, J. Lygeros and S. Sastry (2001). Structural stability of hybrid systems. In: *Proceedings of the European Control Conference*. Porto, Portugal.

Skogestad, S. and I. Postlethwaite (1996). *Multivariable feedback control - analysis and design*. Wiley.

Sumida, T., H. Iwanaga and T. Tahara (2007). Numerical indication of structural stability in dynamical systems and its application to clinical study. *International Journal of Bifurcation and Chaos* **17**(1), 283–291.

Wen, L. (1996). On the C^1 stability conjecture for flows. *Journal of Differential Equations* **129**, 334–357.